VOL. 10, NO 20, NOVEMBER, 2015 ISSN 1819-6608
ARPN Journal of Engineering and Applied Sciences

www.arpnjournals.com

EFFECT OF COOLING RATE IN VARIANT SELECTION DURING BAINITE TRANSFORMATION IN HEAT AFFECTED ZONE OF CR-MO STEEL

Sarizam Mamat[1] and Yu-Ichi Komizo[2]
[1]Faculty of Earth Science, Universiti Malaysia Kelantan, Jeli, Kelantan, Malaysia
[2]Joining and Welding Research Institute, Osaka University, Mihogaoka, Ibaraki City, Osaka, Japan
E-Mail: sarizam@umk.edu.my

ABSTRACT
The effect of the cooling rate on the variant selection mechanism during bainite transformation was investigated in 2Cr-1Mo steel. The specimen was heat treated to 1350 ℃ and held for 60s before being cooled to room temperature with various cooling rates. The usage of high temperature laser scanning confocal microscopy (LSCM) to heat and cool the specimen under controllable conditions enabled the bainite transformation to be observed in a real time. The heat treated sample was then analyzed by using electron backscattered diffraction (EBSD) method. As a result, increasing the cooling rate was discovered to refine the bainite block size. In the higher cooling rates, high angle variants were formed prominently.

Keywords: variant analysis, bainite, phase transformation, heat affected zone, Cr-Mo steel.

INTRODUCTION
Owing to the hope of obtaining the best balance between strength and ductility, bainite has become more important in steel technology nowadays [1], [2]. The weld area can be defined as the area that includes the weld metal and the heat affected zone (HAZ). The coarse grained HAZ is the most affected area during the welding process due to rapid cooling that causes hardening, which in turn is possibly the main factor influencing cleavage fractures.

In order to increase ductility in this area, the stimulated formation of bainitic microstructure is one of the alternatives that are being conceived nowadays to produce a finer microstructure [3]. It is reported that the cleavage fracture resistance of bainitic microstructures is closely related to both prior austenite and bainite packets [4].

In the last few years, several pieces of research have been done to analyze the transformation of upper bainite by means of the electron backscattered diffraction (EBSD) analysis method [5-7]. Until now, the behavior of bainite transformation in the weld area especially the HAZ which is associated with variant analysis of crystallographic packets has scarcely been studied.

Therefore, the aim of this study is to investigate the behavior of bainitic ferrite block formation during transformation, and its correlations with variant selection mechanisms in a single prior austenite grain. The focus of variant analysis here is on the orientation relationships of each block formed with various cooling rates. Thus, the effect of cooling rates on the variant selection mechanism can be identified.

EXPERIMENTAL METHOD
The material used in this experiment was Cr-Mo steel (Fe-0.14%C-2.14%Cr-0.86%Mo wt%). In observation of phase transformations was conducted by using high temperature laser scanning confocal microscopy (LSCM). An elaborate description of LSCM has been detailed in previous research [8], [9]. By using LSCM, the specimens (φ5×1(t)) were heated to 1350 ℃ at a heating rate of 15 ℃/s and held at this temperature for 60s. After that, each specimen was cooled to room temperature at four different cooling rates which are 35 ℃/s, 15 ℃/s, 10.8 ℃/s and 3.3 ℃/s. By this method, the bainite transformation could be observed in real time with a high resolution. The crystal orientation of each heat treated sample was then measured at room temperature by SEM/EBSD. The accelerating voltage of SEM (JEOL JSM-6400) was 20kV and the electron beam diameter was about 0.2μm. The step size was 0.5 for 35 ^{o}C/s, 0.7 for 15 ^{o}C/s and 0.8 for 10.8 ^{o}C/s. Both analysis results were then compared to each other in order to study the behavior of bainite transformation.

RESULTS AND DISCUSSIONS

Transformation behavior
Figure-1 (a) and (b) illustrate the Bain Plane (BP) map and Close-packed Plane (CP) map for the specimen cooled at a 35 ℃/s cooling rate. Then, the BP map and CP map in Figure-1 (c),(d) and Figure-1 (e),(f) respectively refer to the 15 ℃/s and 10.8 ℃/s cooling rate. The black line in both maps refers to the combination of variants with high misorientation angles, while the white line refers to those variants with CSL Σ3 relationships. From the BP map

analysis results, it can be concluded that there is no existence of high misorientation angle variants or twin (CSL Σ3) relationship variants formed in the same correspondence bain area. Meanwhile, based on the CP map analysis result, it was found that there were abundant twin relationships where CSL Σ3 variants formed in the same packet area. By comparing both maps for every condition, even though there were some cases that showed a good correlation between variants in a packet boundary to be in the same bain group (as shown as a blue ellipse in Figure-1 (b), (d), (f)) or connected with low angle misorientation (white line), in most cases, packet boundaries were predominantly connected with a high angle of misorientation (black line).

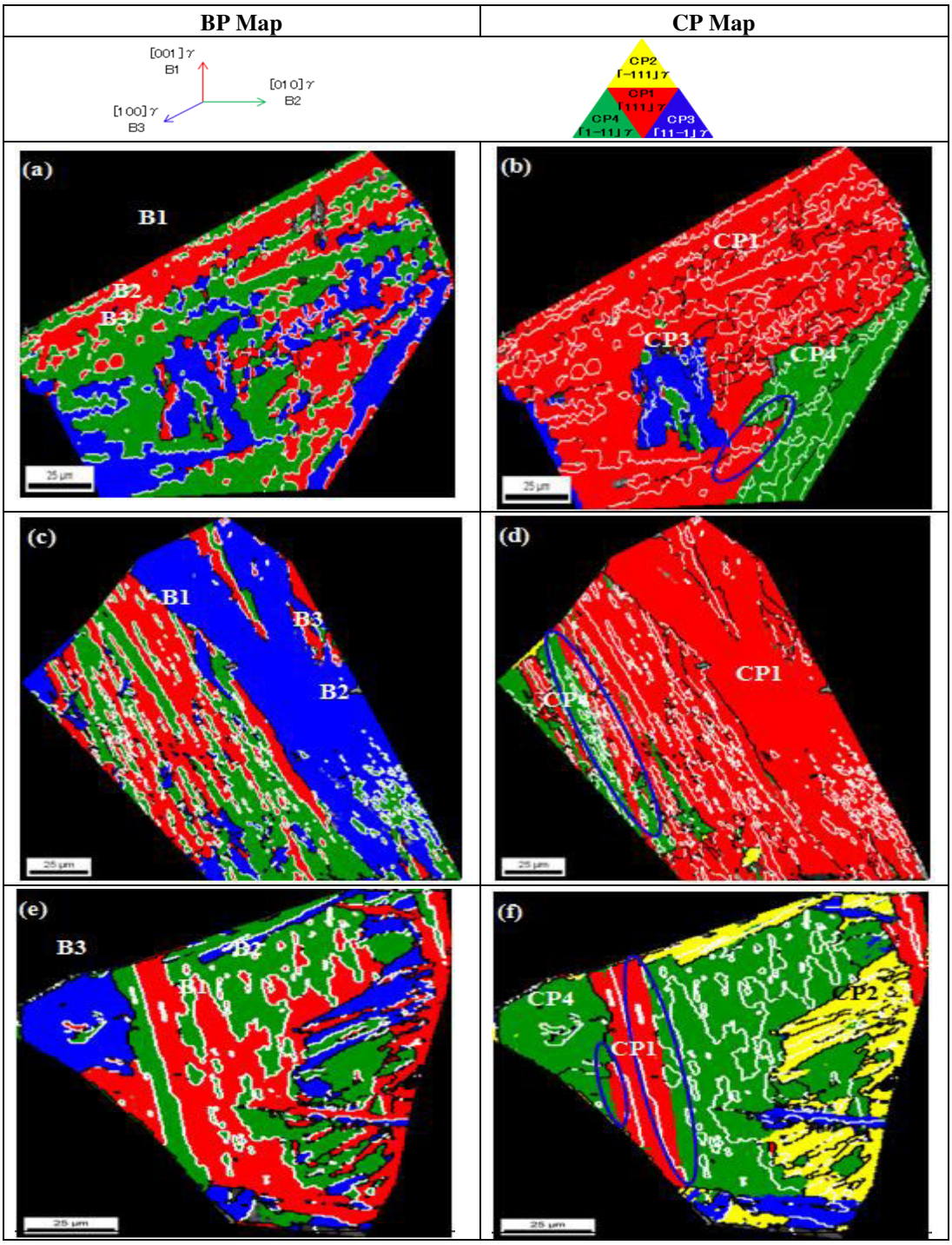

Figure-1. BP map and CP map for each condition: (a), (b) 35℃/s, (c), (d) 15℃/s and (e), (f) 10.8℃/s. The blue ellipse in the CP map refers to the variants in the same bain group formed in a packet boundary.

Correlation between block formation sequences and variants

Figure-2 illustrates the correlations between transformation sequences and the formation of variants in the grain for the case of a 35°C/s cooling rate. By comparing both LSCM and EBSD analysis pictures, the first block (R1) can be matched to V1 which is colored in red. Afterwards, the second block (R2) transformed just next to R1 and it can be matched as V2. Subsequently, it was observed that R3 and R4 transformed simultaneously from two different grain boundaries. These blocks could be matched as V19 in purple and V12 in sky blue colors. From the surface of the block that has been recognized as V19, the V6 which is in the same bain group which nucleates before causing a twinning to form V5 and V2 (V5 and V2 are known to be a variant pair). Nevertheless, R4 is recognized as the V12 which grew in width direction to nucleate V8 that had a misorientation angle of 60° before causing a twinning with V7. Consequently, the last block (R5) which could be matched to V2 seemed to form under the influence of the transformation that occurred in the neighboring grain. The finest microstructure, circled in white on the EBSD analyzed picture was observed to be the last region to transform. The formation of secondary bainite from R3 (V19) was observed and matched to V6, which belongs to the same bain group as V19. From there on, the twinning with V5 was detected which then formed V2 and V7 which is known to be in the same bain group with V5. It was found that the formation of copious variants from the same bain group was one of the mechanisms in strain accommodation during bainite transformation.

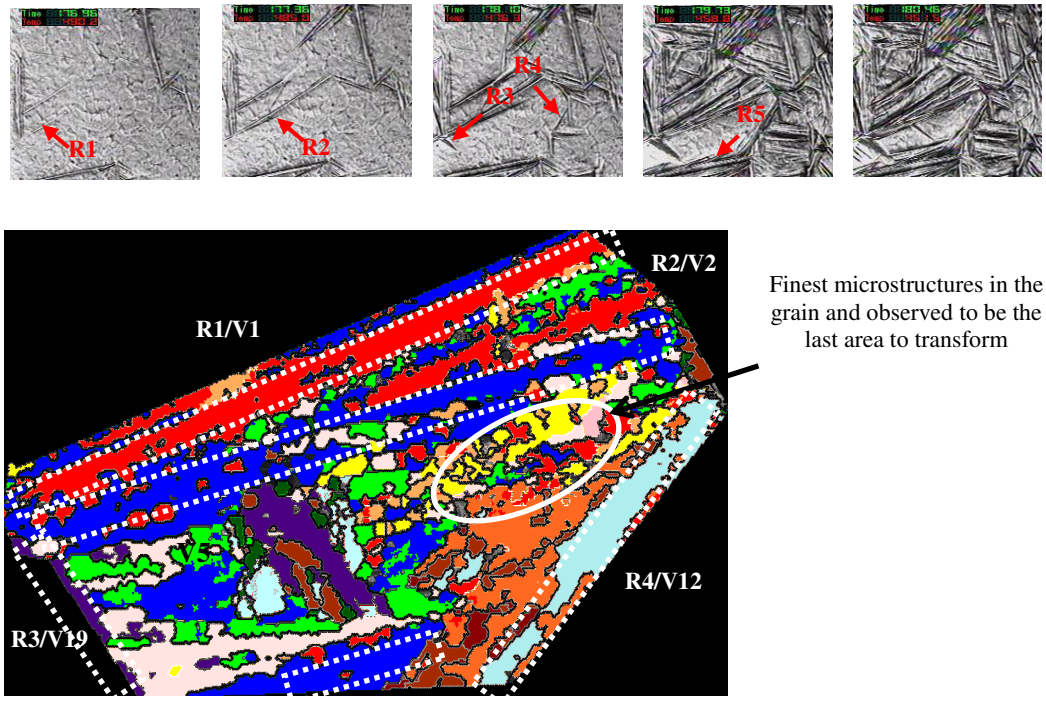

Figure-2. Correlations between transformation sequences by LSCM to be matched with variants formed in the grain for the case of 35 °C/s cooling rate.

Figure-3 illustrates the correlations between transformation sequences and the formation of variants in the grain for the case of a 15°C/s cooling rate. The first block (S1) can be matched to V2, which is yellow in color. The second block (S2) transformed just next to S1 from the opposite grain boundary, and it can also be matched as V2. The third block (S3) which matched as V7 that nucleated adjacent to the V2 block. For V2 and V7 were recorded to have CSL Σ1 relationships and classified to be in different packets. Hereafter, the twinning occurred to the S3 block to form V8 during the growth process. At the same time, the S4 block which can be matched as the V6 is transformed and impinged upon S1. The S5 block then transformed next to S3 and matched as V1. The transformations can be said to abide by some preferential variant selection rules, whereby variants with a twinning relationship transformed during the growth process or between two different blocks within a similar packet. Whereas, variants from the same bain group or having CSL Σ1 relationships formed adjacently when they came to different packets. There was also the formation of secondary bainite which nucleated from the surface of S4 (V6). From the analysis, this afore mentioned secondary bainite was matched as V3 and belonged to the same bain

group as the V6. From there on, the formation of V2 (having a CSL Σ11 relationships with V3) and V1 during development was observed.

Figure-4 illustrates the correlations between transformation sequences and the formation of variants in the grain for the case of a 10.8 ℃/s cooling rate. The first block (P1) could be matched to V2, which then caused twinning to form V1 during the growth process. It grew to the width direction by forming V8 which had a CSL Σ1 relationship with V1, followed by V7 which had a CSL Σ3 relationship with V8. Furthermore, the transformation temperature of this grain was in fact relatively higher than the other two cases. It produces a coarser block in the early stage of transformation, but it became finer at the final stage.

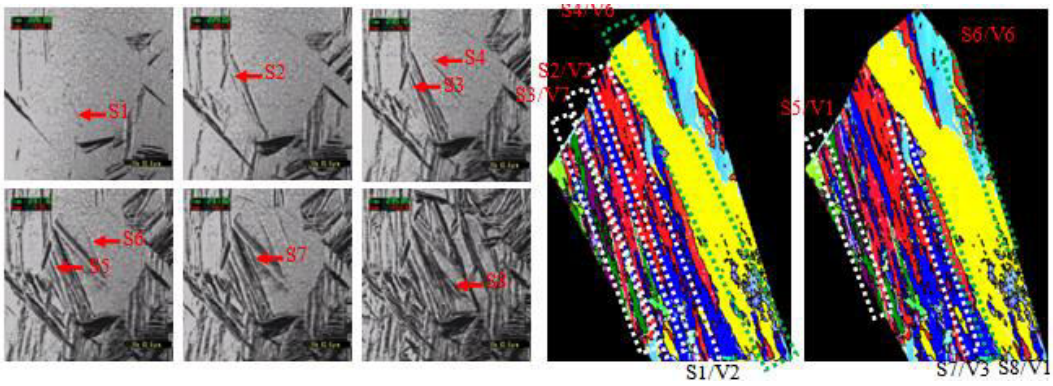

Figure-3. Correlations between transformation sequences by LSCM to be matched with variants formed in the grain for the case of a 15 ℃/s cooling rate.

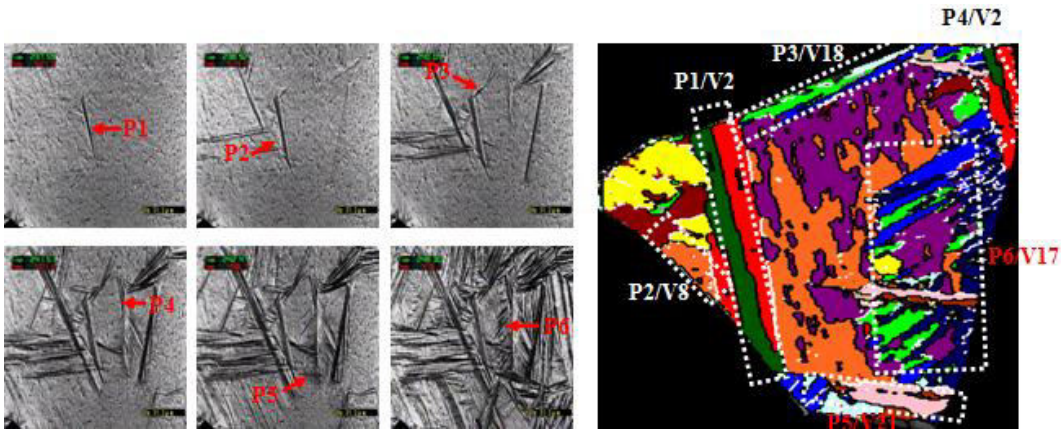

Figure-4. Correlations between transformation sequences by LSCM to be matched with variants formed in the grain for the case of a 10.8 ℃/s cooling rate.

Effect of cooling rates

Table-1 is summarizing the data for the transformation temperature of each cooling rate, including the average block sizes. It is clear that the average block size is decreased by increasing the cooling rate. This result suggests that a finer microstructure of bainitic ferrite can be obtained by imposing a higher cooling rate. Figure-5 shows the fraction of variants which have a CSL relationship, and the line graph shows the tendency to form high misorientation angles for each cooling rate. It is considered that there is an intimate correlation between both increasing block sizes and decreasing the CSL Σ3/ high angle upon decreasing the cooling rates. During bainite transformation, it has been demonstrated that the transformation develops by two mechanisms such as the plastic-accommodation which normally occurs at high temperatures and self-accommodation at low temperatures [12]. Bainite transformation during continuous cooling involves both mechanisms. Due to rapid cooling, the carbon in the austenite phase remains in saturated conditions. However, as part of the transformation progress, the carbon will escape out from the bainitic ferrite block since the transformation occurs at a higher temperature compared to martensite. This will divide the austenite region into two different carbon concentrations-carbon-enriched, and carbon depleted regions-and the block of bainitic ferrite then has to grow from the carbon depleted area [10, 11]. Hereafter, any excess carbon is

soon partitioned into the vicinity of residual austenite or else precipitates as carbides. The amount of bainite that forms increases as the temperature decreased. Nonetheless, the faster the drop in temperature, the shorter the diffusion time for the carbon to move. Hence, the carbon remains in homogeneous conditions which then produce many sites for the nucleation of bainitic ferrite. These conditions in turn refine the size of bainitic ferrite block. An expulsion of carbon to the surrounding austenite after the formation of the bainitic ferrite block thermodynamically stabilizes the austenite for further transformation. Due to the large undercooling, the increment in the driving force then initiates the formation of adjacent bainitic ferrite blocks. Nevertheless, the austenite is in a stable condition. As shown in Figure-1, it could be verified that most of the variants formed adjacently had either a twinning relationship or a high angle of misorientation. In fact, the twinning phenomenon in steels is well known to have a close relationship to the plasticity of deformation. The formation of twinning during transformation can here be attributed to this plastic-deformation, and it is suggested that the formation of this twinning is to accommodate the transformation plastically. However, the formation of CSL Σ3 was decreased by smaller undercooling. This increase in the fraction of variants with low angles of misorientation (including Σ1). By reducing undercooling is a result of better variant selection which then allows individual plates to grow larger and coarsen the bainitic ferrite block. As a continuation of the above discussion, the twinning between blocks in the same packet is a common condition in all cooling rates. The packet boundary that was observed to form during reduced undercooling was normally connected with low misorientation angle variants from the same bain group, yet high angle variants tended to form in during stronger undercooling (refer Figure-1). It is reported that the combination of variants from the same bain group formed in the packet boundaries was able to accommodate the strain transformation [12-14]. However, in the case of relatively low temperature transformation (in both cases, whether the undercooling was strong or weak), the amount of untransformed austenite is reduced. Due to a high transformation driving force, the difference in the activation energy for nucleation between bainitic ferrite variants should be smaller. More variants which able to nucleate [15] will resulting in the high angle packet boundaries. The same explanation is applicable to the last transformed area in the formation of the fine bainitic ferrite block. As shown in Table-1, the transformation starting temperature for 35 ℃/s was the lowest. It is suggested that this is one of the reasons for this result, rather than the cooling rate factor.

Table-1. Effect of cooling rate upon the average block size.

Cooling rate [℃/s]	**Transformation start temperature** [℃]	**Transformation finished temperature** [℃]	**Transformation period** [s]	**Average block size** [μm]
35	512	409	9	1.95
15	535	420	28	2.82
10.8	533	452	20	3.59

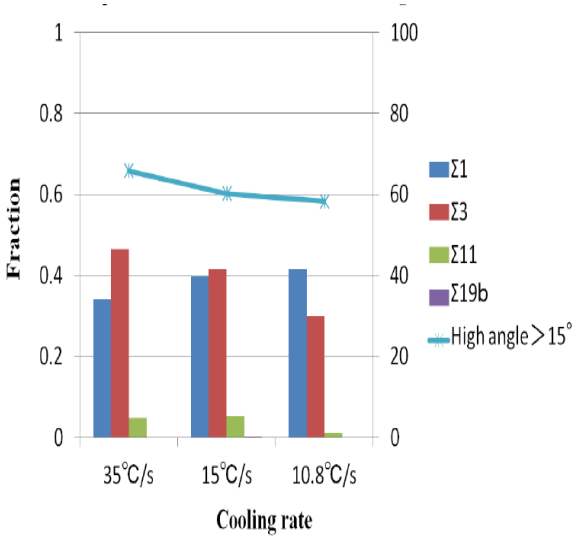

Figure-5. Relationship between fraction of variant.

CONCLUSIONS

In this study, observation was concentrated upon the transformation of bainite in a single austenite grain. The transformation sequence within the grain was analyzed. By using the EBSD method, the orientation relationship of each transformed block was analyzed. Comparing these two results, the main conclusions pertaining to bainite transformation behavior in Cr-Mo steel are as follows:

1) There is no formation of high misorientation angle variants in the same correspondence bain area. However, the twinning relationship (CSL Σ3) variants seem to be transformed in the same packet area. The packet boundary is connected with variants which have a high misorientation angle.
2) The formation of high angle variants during bainite transformation is very prominent in higher cooling rates. Formation of CSL Σ3 is identified as a main

factor for this behavior. This is subject to plastic-deformation within the austenite phase in order to accommodate the transformation.

3) An increment of the cooling rates refines the bainitic ferrite block.

REFERENCES

[1] Barbacki. 1995. The role of bainite in shaping mechanical properties of steels. Journal of Materials Processing Technology. 53 (1): 57-63.

[2] Bhadeshia H. K. D. H. and Christian J. W. 1990. Bainite in steels. Metallurgical transactions A. 21(3): 767-797.

[3] H. K. D. H Bhadeshia. 1999. Some phase transformations in steels. Materials Science and Technology. 15(1): 22-29.

[4] A. Lambert-Perlade, A. F. Gourgues and A. Pineau. 2004. Austenite to bainite phase transformation in the heat affected zone of a high strength low alloy steels. Acta Materialia. 52(8): 2337-2348.

[5] T. Furuhara, H. Kawata, S. Morito and T. Maki. 2006. Crystallography of upper bainite in Fe-Ni-C alloys. Materials Science and Engineering A. 431(1): 228-236.

[6] S. Morito. 2009. Crystallographic characterization of lath martensite and upper bainite. Fueramu. 14(2): 28-33.

[7] G. Miyamoto, N. Iwata, N. Takayama and T. Furuhara. 2012. Variant selection of lath martensite and bainite transformation in low carbon steel by ausforming. Journal of Alloys and Compounds. 577(1): S528-S532.

[8] Y. Komizo and H. Terasaki. 2011. Optical observation of real materials using laser scanning confocal microscopy: Part 1-techniques and observed examples of microstructural changes. Science and Technology of Welding and Joining. 16(1): 56-60.

[9] Y. Komizo and H. Terasaki. 2011. Optical observation of real materials using laser scanning confocal microscopy: Part 1-techniques and observed examples of microstructural changes. Science and Technology of Welding and Joining. 16(1): 56-60.

[10] Z. Ławrynowicz and A. Barbacki. 2002. Features of bainite transformation in steels. Advances in Materials Science. 2(1): 5-32.

[11] S. S. Babu, E. D. Specht, S. A. David, E. Karapetrova, P. Zschack, M. Peet and H. K. D. H. Bhadeshia. 2005. In-situ observations of lattice parameter fluctuations in austenite and transformation to bainite. Metallurgical and Materials Transactions A. 36(12): 3281-3289.

[12] S. Zhang, S. Morito and Y. -I. Komizo. 2012. Variant selection of low carbon high alloy steel in an austenite grain during martensite transformation. Iron and Steel Institute of Japan International. 52(3): 510-515.

[13] A. Lambert-Perlade, A. -F. Gourgues and A. Pineau. 2004. Austenite to bainite phase transformation in the heat-affected zone of a high strength low alloy steel. Acta Materialia. 52(8): 2337-2348.

[14] T. Furuhara, H. Kawata, S. Morito and T. Maki. 2006. Crystallography of upper bainite in Fe-Ni-C alloys. Materials Science and Engineering A. 431(1): 228-236.

[15] T. Furuhara, H. Kawata, S. Morito, G. Miyamoto and T. Maki. 2008. Variant selection in grain boundary nucleation of upper bainite. Metallurgical and Materials Transactions A. 39(5): 1003-1013.